Chemical Physics 357 (2009) 181–187

Contents lists available at ScienceDirect

Chemical Physics

journal homepage: www.elsevier.com/locate/chemphys

Carotenoid deactivation in an artificial light-harvesting complex via a vibrationally hot ground state

Janne Savolainen [a,*], Tiago Buckup [b], Jürgen Hauer [c], Aliakbar Jafarpour [a], Carles Serrat [d], Marcus Motzkus [b], Jennifer L. Herek [a]

[a] Optical Sciences Group, Department of Science and Technology, MESA+ Institute for Nanotechnology, University of Twente, 7500 AE Enschede, The Netherlands
[b] Physikalische Chemie, Fachbereich Chemie, Philipps-Universität, D-35032 Marburg, Germany
[c] Institut für Physikalische Chemie, Universität Wien, A-1090 Vienna, Austria
[d] Tecnologies Digitals i de la Informació, Universitat de Vic, E-08500 Vic, Spain

ARTICLE INFO

Article history:
Received 8 August 2008
Accepted 5 January 2009
Available online 10 January 2009

Keywords:
Artificial light-harvesting
Carotenoid deactivation
Ultrafast spectroscopy
Energy transfer
Excitation energy dependence

ABSTRACT

Ultrafast relaxation of a carotenoid in an artificial light-harvesting complex has been studied by transient absorption spectroscopy. The transient signal amplitudes at several wavelengths as well as the amplitudes of the underlying species associated spectra (SAS) are analysed for several excitation energies ranging over more than two orders of magnitude (10 nJ/pulse up to 3000 nJ/pulse). Our analysis shows that the contribution from the so-called S^* signal on the long-wavelength side of the first allowed $S_0 \rightarrow S_2$ transition has a markedly different excitation energy dependence and saturation behaviour than the electronic excited state S_1. These observations are modelled and explained in terms of a two-photon excitation of a vibrationally hot ground state via an impulsive stimulated Raman scattering (ISRS). The experimental observations of the varying pulse energy dependencies of different excited state species are supported by an analysis based on a density-matrix formalism.

1. Introduction

Carotenoids are abundant biomolecules that perform several essential tasks in the photosynthetic molecular machinery in Nature. One of the functions of carotenoids is to interact with photons in the blue–green region of sunlight and subsequently pass the absorbed energy forward to porphyrin molecules in various natural light-harvesting antenna complexes. A great amount of work has delivered knowledge with increasing detail on the photophysics of carotenoids as well as the many roles they play in the photosynthetic light-harvesting complexes [1]. Recently, much interest has been directed to the details of the deactivation pathways of carotenoids that follow excitation by ultrashort laser pulses. More specifically, considerable interest in carotenoid reaction dynamics has been shifted to the presence and role of additional (intermediate) excited states.

The generally accepted energy-level scheme of carotenoids comprises a ground state $S_0(1A_g^-)$ linked to the state $S_2(1B_u^+)$ via the first optically allowed transition. Upon excitation, S_2 relaxes via a rapid internal conversion process towards the S_1 state $(2A_g^-)$. The transition $S_0 \rightarrow S_1$ is symmetry forbidden. Nevertheless, in recent years due to new experimental findings, afforded by the increased availability of ultrafast laser pulses in the visible region, this comprehensive picture of carotenoid deactivation has been refined, and more elaborate models have been put forward. Predominantly, the current discussion relates to an additional long-lived spectro-temporal contribution in transient absorption spectra that is red shifted with respect to the observed linear absorption band; the $S_0 \rightarrow S_2$ transition. This spectro-temporal feature, sometimes referred to as S^*, depicts a behaviour different from that of the other resolved transient spectra assigned to electronic excited states [1–5].

The interpretation of such experimental results relies strongly on the theoretical predictions made by Tavan and Schulten some 20 years ago for short polyenes with 4–12 π-electrons [6,7]. These calculations predicted the electronic energies for all four possible low-lying excited electronic states of linear polyenes ($1B_u^-$, $1B_u^+$, $2A_g^-$, and $3A_g^-$). Consequently, the involvement of such additional electronic dark states in the photophysics of carotenoids has been studied in several theoretical and experimental works, and some studies show good correlations between theory and experimental findings [8], whereas other studies show deviations as large as 30%.

Both sequential and parallel relaxation pathways have been proposed that involve one or more additional dark electronic

* Corresponding author.
E-mail address: janne.savolainen71@gmail.com (J. Savolainen).

0301-0104/$ - see front matter © 2009 Elsevier B.V. All rights reserved.
doi:10.1016/j.chemphys.2009.01.002

state(s) between the S_2 and S_1 states [9], depending on the conjugation length of the carotenoid. For carotenoids longer than 11 conjugated double bonds, it was suggested that two additional dark states ($1B_u^-$ and $3A_g^-$) are involved in a sequential relaxation from initially excited S_2–S_1, while in shorter carotenoids, just $1B_u^-$ would participate [8,10]. In a study on a series of carotenoid zinc phthalocyanine dyads, the discussed energy-flow diagram included S^* as an independent intermediate electronic state between S_2 and S_1 [11]. In another set of experiments, the aforementioned S^* state was associated with a precursor state for triplet formation in light-harvesting complexes [12,2,13,14]. Further, speculations that S^* could be the $1B_u^-$ state predicted by theory have been presented [2,15]. However, as pointed out by Niedwiedzki et al. [5] such an assingment is problematic; since the strongly allowed transition associated with the S^* band should reach an A_g^+ state, this would put the energy of the proclaimed S^* state below the known successor state S_1. Furthermore, several studies recently have shown that such intermediate dark states are not required in the $S_2 \rightarrow S_1$ deactivation [16,3,17–19]. These discrepancies between theory and experiments have prompted other interpretations for carotenoid deactivation. The suggested schemes include ground state heterogeneity [4], an ultrafast isomerization [20,5,21,22], and a vibrationally hot ground state [23,16,3].

In a previous study, we used transient absorption spectroscopy to investigate the photophysics of an artificial light-harvesting dyad that comprises a carotenoid and a purpurin molecule that are covalently linked with an amide linker (see Fig. 1a, inset) [24]. The caroteno-purpurin dyad is a model system designed to mimic the salient features of the natural light-harvesting complex LH2 from the purple bacterium *Rhodopseudomonas acidophila*, while preserving structural simplicity [25]. The caroteno-purpurin dyad and related compounds based on the principles of biomimicry have proved to be promising molecular systems for applications of artificial light-harvesting [26,27] as well as for the purposes of fundamental research aiming to shed light on the fundamental photophysics of the early events of light-harvesting [28,24] and in coherent control experiments [29].

Using global data-analysis techniques, we resolved the energy-level diagram, energy-flow pathways, the associated rate constants, and species associated spectra (SAS) from experimental data. Briefly (see also Fig. 1b), after excitation at 510 nm, energy transfer (ET) from the carotenoid S_2 state to purpurin takes place in 50 fs. Simultaneously, the first excited state (S_1) of the carotenoid is populated via a vibrationally hot S_1 state by a competing internal conversion (IC) process in 110 fs, resulting in a 30/70 branching ratio between IC and ET. The vibrational cooling of the S_1 state takes approximately 290 fs, and is followed by a decay to the ground state in 7.8 ps. The lowest excited energy-level of the purpurin is deactivated on the nanosecond time scale to its ground state or via inter-system crossing and triplet–triplet energy transfer processes to carotenoid triplet state. The model used in target analysis that best fits the data also includes a hot ground state that gains population within the duration of the ultrafast pump pulse by an impulsive stimulated Raman scattering (ISRS) process. Furthermore, we concluded that the major differences between the photophysics of the dyad molecule and LH2 are in the deactivation network of the carotenoid moiety, which is consistent with the photophysics of carotenoids in solution rather than in the protein environment of the LH2 complex.

In this contribution, we use the dyad molecule to further investigate the carotenoid deactivation in the artificial light-harvesting complex. We do this by an energy dependence study of transient absorption signals, where the energy of the excitation pulse is varied by more than two orders of magnitude.

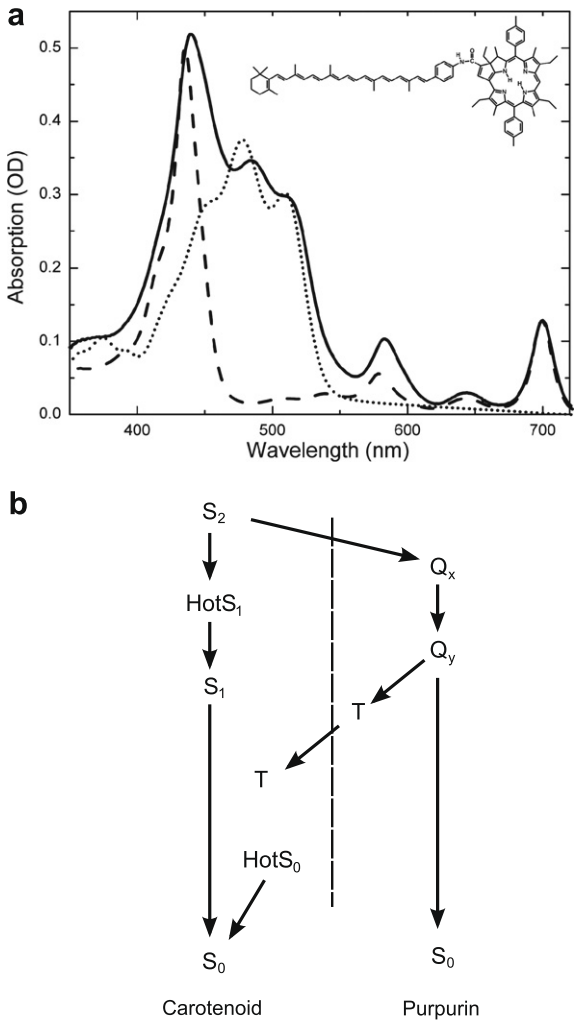

Fig. 1. Artificial light-harvesting complex. (a) Structure (inset), and absorption spectra of the dyad (solid line), carotenoid (dotted line), and purpurin (dashed line). (b) The simplified energy-level diagram showing deactivation pathways.

2. Experimental section

The pump–probe setup has been described earlier [24]. In brief, part of the output of an amplified Ti:Sapphire (CPA-2001, Clark-MXR, Inc.) laser was coupled into a noncollinear optical parametric amplifier (NOPA, Clark-MXR, Inc.), which produced ~10 μJ near-transform-limited pulses at the centre wavelength of 510 nm with a FWHM bandwidth of 28 nm and an 18 fs pulse duration to be used as the pump pulses. For probing, white-light continuum pulses, ranging spectrally from 450 to 710 nm, were created by focusing a small fraction of the laser output into a sapphire window. The polarisation angle between the pump and the probe pulses was set to the magic angle (54.7°) to avoid any anisotropy effects. The two beams were focussed and overlapped at the sample position, where the FWHM diameter of the Gaussian intensity profiles of the pump and probe beams were 220 and 40 μm, respectively. The pulse energy was set with an adjustable filter in the pulse energy range of 10 nJ–3 μJ. The sample cuvette was rotated sufficiently quickly to provide a fresh sample volume for every pulse in order to avoid sample degradation or accumulation of long-living states. The probe pulses were coupled via a spectrograph (Acton-SP2150i; Princeton Instruments, Inc.) onto a home-build 256-pixel diode array.

The time resolution of the pump-probe experiments as well as the amount of spectral dispersion in the WLC were determined by measuring the sum-frequency-mixing signal of the pump and probe pulses at the sample position in a 25 μm-thick BBO crystal. The wavelength to be mixed from white-light continuum was selected by tuning the phase matching angle of the crystal. In this way, the mixing of different wavelengths of the WLC could be measured. The time resolution was ~60 fs across the spectrum, and the overall time delay between the blue and red parts of the WLC spectrum (chirp) was approximately ~300 fs. The measured chirp curve was used to remove the WLC dispersion from the data prior to analysis.

The caroteno-purpurin dyad was prepared using published procedures [30]. Spectroscopy-grade toluene was purchased from Riedel-DeHaën and used without further purification. Optical density at 510 nm was ~0.3 OD in a rotating cuvette having a 0.5 mm optical path length. To check for any sample degradation, the steady-state absorption spectrum was measured before and after the measurements. No changes in the OD or spectral shapes were observed, indicating sample stability. All measurements were carried out at room temperature.

3. Results

We varied the energy of the pump pulse while monitoring the transient absorption signals belonging to different spectral channels. Fig. 2 shows energy-scan traces for four spectral regions of interest based on the previously resolved species associated spectra (SAS) [24]. Each trace represents a 5-nm integrated region centred at the maxima of the following signals: carotenoid bleach (480 nm), carotenoid S^* (540 nm), carotenoid S_1 (610 nm), and purpurin bleach (700 nm).

Generally for any two-level system, the saturation of a resonant transition is described by a simple first-order differential equation that can be solved to its single exponential form $f(E) = b(1 - e^{-E/E_{Sat}})$. In the impulsive limit, with ultrafast laser pulses and omitting any relaxation times, this holds and E_{Sat} is simply proportional to the inverse of the sum of the cross sections σ_{01} (absorption) and σ_{10} (stimulated emission); $E_{Sat} \propto (\sigma_{01} + \sigma_{10})^{-1}$. With a centre wavelength of 510 nm, a beam diameter of 220 μm, a molar extinction coefficient of $5 \times 10^4\ M^{-1}\ cm^{-1}$, and assuming equal σ_{01} and σ_{10}, the saturation fluence Fl_{Sat} is found to be 2.6×10^{15} photons cm^{-2} corresponding to $E_{Sat} \sim 385$ nJ/pulse. However, a single exponential function expected for a saturation of a resonant one-photon transition fails to describe the energy-scan traces adequately. A better fit is found by adding an extra linear contribution using the following function:

$$F(E) = aE + b(1 - e^{-E/E_{Sat}}), \quad (1)$$

where E is the pulse energy in nJ; a and b are free fitting parameters; and E_{Sat} is a global variable common to all four traces. As can be seen from the data (symbols) and the fit (grey lines) in Fig. 2, all traces are well described with this function. The fit gives the global 'saturation-energy' variable E_{Sat} a value of ~410 nJ/pulse, which is in good agreement with the approximated value of 385 nJ/pulse. The slope of the linear part (free parameter a) varies substantially from channel to channel. S^* and PT have the steepest slopes (0.0072 and 0.0040, respectively), S_1 a slight one (0.0018), and purpurin bleach has zero linear contribution. The additional term aE used in the fitting function (Eq. (1)) is basically a linear approximation of another exponential term, hence it describes a deviation from the simple two-level excitation scheme. The resulting slopes of the linear contributions in the chosen four spectral channels describe to what extent each recorded signal deviates from the simple single exponential saturation model. The purpurin bleach is unaffected ($aE = 0$) and S_1 requires only a very small slope, whereas the carotenoid bleach and especially the excited state absorption at the proposed spectral region of S^* require significant contribution for adequate fits.

As expected, these features manifest themselves spectrally as well. Fig. 3 shows how the shape of the transient spectrum at 1 ps varies with the energy of the pump pulse. The spectra are normalised at the peak of the S_1 excited state absorption (ESA) signal at 610 nm. Relative to the S_1 ESA, the negative carotenoid bleach signal in the blue end of the spectrum increases; the 'shoulder' at the red side of the ground state absorption grows; and the negative purpurin bleach signal at ~700 nm decreases. Qualitatively, the intensity-scan data indicate that while the $S_0 \rightarrow S_2$ transition appears to saturate, the other channels, especially S^*, remain active and continue to gain population.

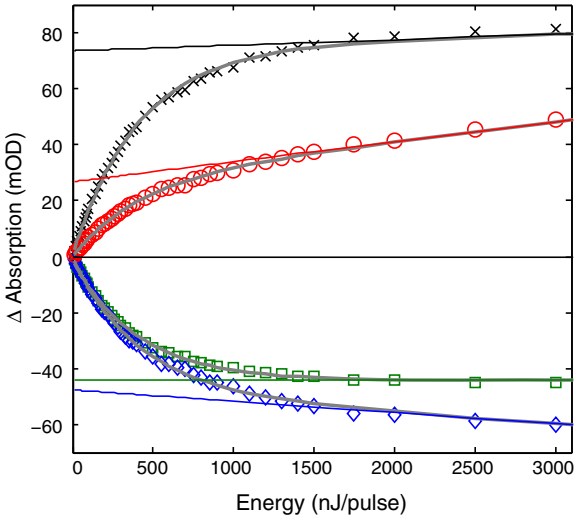

Fig. 2. Linearity curves for the chosen spectral channels at 1 ps. Carotenoid bleach at 480 nm (blue diamonds), carotenoid S^* at 540 nm (red circles), carotenoid S_1 at 610 nm (black crosses), and purpurin bleach at 700 nm (green squares). Grey lines show the fitting results. The coloured lines show the linear contributions found in the fit.

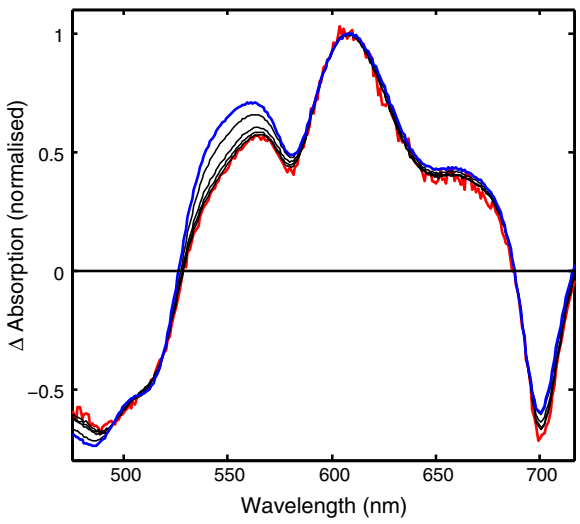

Fig. 3. Normalised transient spectra with increasing pump intensity. 20 (red), 140 (black), 350 (black), 800 (black), 2000 (black), and 3000 (blue) nJ/pulse. The spectra are normalised at 610 nm.

A more analytical picture of the energy dependence of the transient spectral features arises when we decompose the measured spectra to the constituting SAS [24] and analyse the changes of the individual contributions (see Fig. 4a). The transient spectrum at 1 ps has no contribution from the S_2 state due to its ultrashort lifetime (<40 fs). Similarly, the T_{Car} signal is absent because no population has yet accumulated into the triplet state at 1 ps probe delay. Thus, we omitted these two contributions and used the remaining six SAS to fit the normalised experimental energy-dependent transient spectra. In the fit, the shapes and the spectral positions of the SAS are kept constant, and only the energy-dependent scaling factors are left to vary as fitting parameters. Fig. 4a shows the scaled spectra for the minimum (10 nJ/pulse, dashed lines) and maximum (3000 nJ/pulse, solid lines) energies, while panels (b) and (c) show the scaling factors found for a range of pump energies. The SAS used are as follows: the carotenoid bleach (Bl_{Car}), ESA from vibrationally hot and relaxed S_1 state ($HotS_1$ and S_1, respectively), and the carotenoid S^*; the SAS belonging to the purpurin moiety are: the purpurin bleach (Bl_{Pur}) and ESA from the Q_y state. Panels (b) and (c) show how the carotenoid $HotS_1$ and S_1 signals stay approximately constant due to the normalisation, whereas the relative caronoid bleach, and especially the S^* signals keep growing with increasing pump energy. Note that the spectrum of S^* was obtained by global target analysis according to the energy-flow diagram presented in the Fig. 1b,

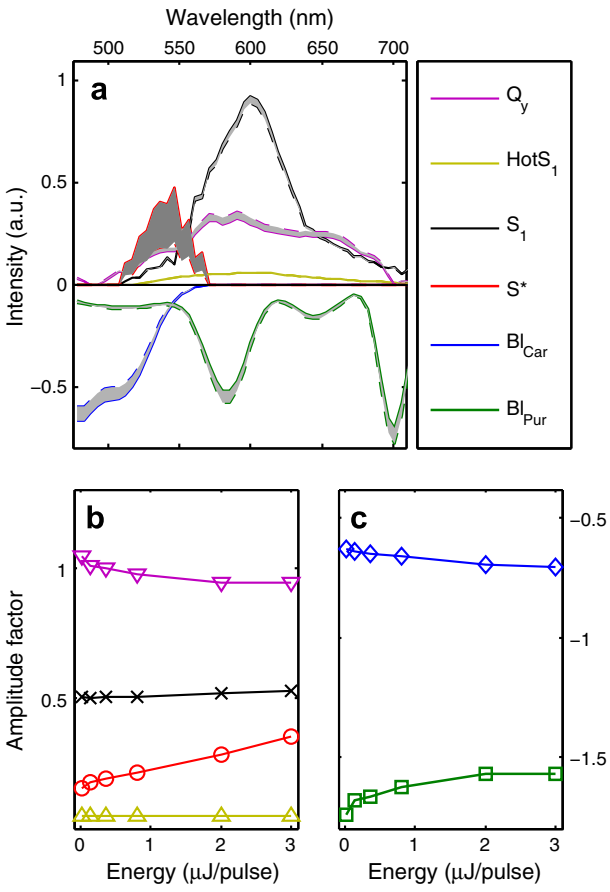

Fig. 4. SAS and pump intensity dependence of the relative scaling factors of the SAS-fitted to the normalised transient spectra. (a) SAS 20 nJ/pulse (dashed lines) and 3000 nJ/pulse (solid lines). (b) The relative amplitude factors for the SAS, positive signals Q_y (magenta triangles pointing down), $HotS_1$ (brown triangles pointing up), S_1 (black crosses), and S^* (red circles). (c) The relative amplitude factors for the SAS, negative signals Bl_{Car} (blue diamonds), and Bl_{Pur} (green squares).

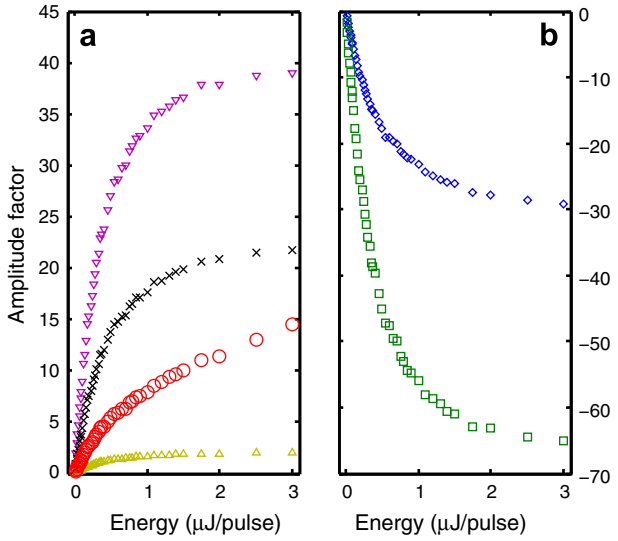

Fig. 5. Pump intensity dependence of the scaling factors of the SAS fitted to the transient spectra. (a) Amplitude factors for the SAS for the positive signals: Q_y (magenta triangles pointing down), $HotS_1$ (brown triangles pointing up), S_1 (black crosses), and S^* (red circles). (b) The amplitude factors for the SAS for the negative signals: Bl_{Car} (blue diamonds), and Bl_{Pur} (green squares).

which assigns it to the vibrationally hot ground state ($HotS_0$). The relative amplitudes of the signals belonging to the ET acceptor species reduce and come to saturation.

Looking at all the measured pump energies, Fig. 5 shows how the amplitude factors evolve when the fit is performed to the original (not normalised) data. Fig. 5 shows how the experiment covers the initial linear regime (0–100 nJ/pulse), and the nonlinear regime (100–3000 nJ/pulse) up to a near-complete saturation of the carotenoid $S_0 \rightarrow S_2$ transition. A striking difference between the carotenoid bleach and S^* signals compared to all the other signal is evident also here: the amplitude scaling factors of carotenoid bleach and S^* continue to grow with increasing pulse energy.

4. Discussion

We have shown how the previously reported transient absorption signals depict different pump energy dependencies, and how this can be roughly explained by an additional excitation process, which is described as an extra linear term in the function describing the signal saturation behaviour. The spectral channel on the red side of the ground state absorption band has the most pronounced contribution of this additional excitation process. Furthermore, we analysed the energy dependence data using previously resolved SAS and showed how the S^* behaviour deviates strongly from the other signals.

From the energy-scan data and the fit using SAS, it becomes evident that relative to the S_1 population, the overall population transfer increases, and an increasingly larger proportion of this extra excited population is directed to the S^* state as the pump energy grows higher. As a consequence, a smaller fraction is available for the ET pathway, which is manifested by the relatively decreasing acceptor (purpurin) bleach and Q_y signals compared to the increasing population transfer to the higher state of the donor (carotenoid). The carotenoid bleach grows as more population is transferred to S^* even after the observed near-complete saturation of the $S_0 \rightarrow S_2$ transition. This indicates that in the artificial light-harvesting dyad, independent of the origin of the signal on the red side of the ground state absorption band, no energy transfer occurs from this state to the acceptor states.

We now proceed by discussing three proposed models for carotenoid deactivation that all aim to explain the differing behaviour of the discussed S^* spectro-temporal signal. The energy-flow diagrams of the three discussed models are shown in Fig. 6: (a) photoisomerization, (b) two-photon absorption to higher state and subsequent ultrafast relaxation to S^* that is an electronic excited state, and (c) model including a hot ground state ($HotS_0$) populated by the ISRS process.

(a) *Photoisomerization.* Recently, it was proposed that xanthophylls (e.g. zeaxanthin and lutein) relax into two different conformers after being excited to the S_2 state [5,21]. This interpretation was also supported by work where transient signals of long-chain xanthophylls were recorded at 77 K, indicating a temperature dependence of the S^* yield [22]. A simplified representation of the model proposed in these studies with the added purpurin energy-levels is shown in Fig. 6a. This branched decay pathway would lead the population of a 6-s-*cis* form and a 6-s-*trans* form associated to a S_1 and the S^*, respectively, and would explain the different relaxation time scales observed for these two components. However, in the light of previous results on energy-flow pathways and related time constants [24], the reported rate constant for the $S^* \rightarrow S_1$ pathway appears slow, up to 120 ps, compared to the S^* 8.8 ps life time found in the dyad [24]. Given that polyene chain length and substituents are essential factors for the observations of Cong et al. [22], one should be cautious in comparing such a small effects between different classes of linear polyenes; carotenoids and xanthophylls. Thus, the $S^* \rightarrow S_1$ channel is likely to be negligible in our polyene. Also, the proposed photoisomerization model is not able to explain how an isomerization process involving such large-scale structural motions could take place in less than 170 fs, which is a typical S_2 lifetime of β-carotene in solution [1]. Nor can the model explain how the process could occur even faster in the case of the dyad having a shorter S_2 lifetime, or in longer carotenoids having even shorter S_2 lifetimes like those observed for the artificial homologues of β-carotene with 13 and 15 conjugated double bonds, where the S_2 relaxes in less than 100 fs [16]. For instance, for molecules of similar size such as retinal in bacteriorhodopsin, the isomerization takes place in ~500 fs in the protein environment [31] and in a few picoseconds in solution [32]. Furthermore, the isomerization model for carotenoids is not in agreement with previous experimental results using a modified transient absorption technique pump-depletion-probe (PDP) [3,16]. In these works, PDP was applied to several open-chain natural as well as artificial carotenoids. The results showed that the absorption change assigned to the S^* channel was independent of the depletion of the S_2 population by an additional depletion pulse tuned to the $S_2 \rightarrow S_n$ resonance at 900 nm [33,8], and immediately following the pump pulse [16]. Such an observation indicates that independent of the origin of the S^* signal, S^* cannot be directly populated from the S_2 state via a relaxation channel within the experimental resolution of ~35 fs. Finally, when applying the carotenoid photoisomerization model to the artificial light-harvesting dyad a question arises: Why would higher energies result in a more efficient relative photoisomerization?

According to Cong et al. [22], upon cooling, the S^* spectrum narrows and its peak shifts to red wavelengths. This can only concur with the findings reported here if one allows for conformational disorder in the ground state, a feature also discussed Papagiannakis et al. [4]. It might be possible that the two-photon process suggested by our intensity dependent data is linked to a conformational sub-population which is not an energetic global minimum. Hence, the conformer favouring the observed two-photon dependence becomes depopulated upon freezing. However, in the study on the caroteno-purpurin dyad molecule fluorescence up-conversion anisotropy measurements indicated the existence of a dominant conformer [30]. This finding was also supported by molecular modelling. Hence, one might argue that in the dyad molecule it is unlikely for large sub-populations to exist.

(b) *Two-photon absorption to higher states.* Another deactivation model for carotenoids has been presented that includes an additional electronic excited state labelled S^*. The involvement of such a dark state has been introduced for spirilloxanthin in solution and in the light-harvesting complex LH1 from the purple photosynthetic bacterium *Rhodospirillum rubrum* [12] and in spheroidene in LH2 from *Rhodobacter sphaeroides* [2]. This model has been further investigated in an intensity study of carotenoid deactivation in rhodopin glucoside in LH2 from *Rhodopseudomonas acidophila* [4]. In this study, S^* as a dark state is further refined by suggesting a new two-photon excitation pathway to a higher-lying electronic excited state, from where a rapid relaxation would transfer population to the so-called S^* dark electronic state. As in the present contribution, the main experimental observation in this study has been the different pump energy dependence of S^* rather than those of the other contributing signals. An adaptation of the suggested model to the dyad is shown in Fig. 6b. A clear two-photon dependence was observed neither for the experimental signal nor

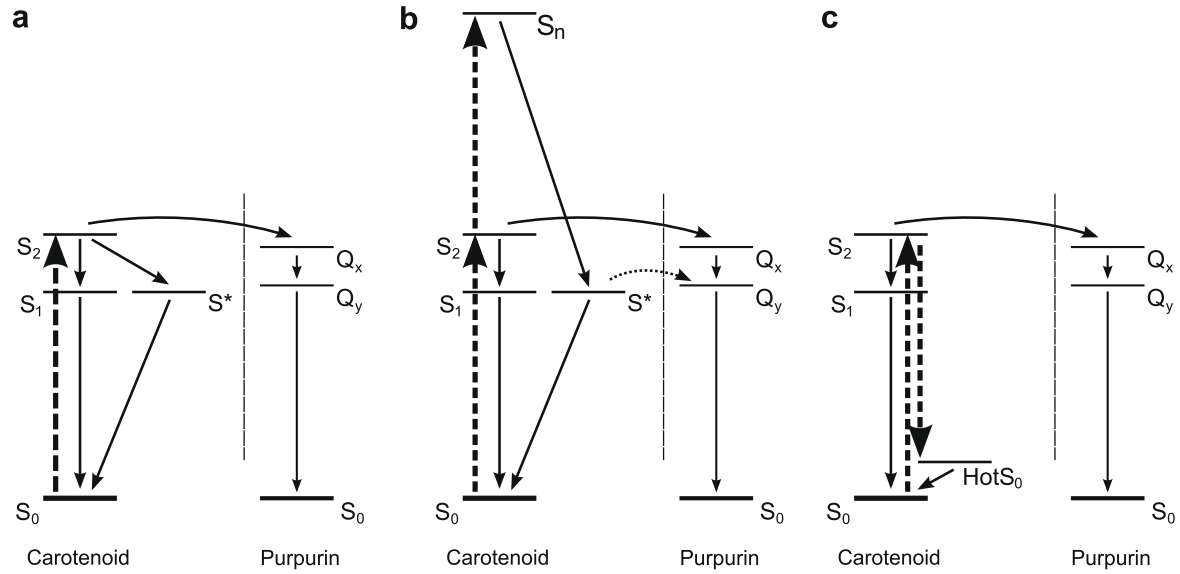

Fig. 6. Three different discussed energy-flow diagrams. (a) Photoisomerization. (b) Two-photon absorption to higher S_n states. (c) Hot ground state model.

for the resolved species associated difference spectrum (SADS) that includes the S^* and bleach signals, indicating a resonant two-photon process [4]. Such a model including a resonant two-photon process relies strongly on the assumption that there is an excited state absorption at the pump wavelength from S_2 to higher-lying states. However, such a resonance has never been reported, whereas a $S_2 \rightarrow S_n$ band has been reported to exist around 900 nm [8].

In a study on molecules closely related to the one under the present study, a series of carotenoid zinc phthalocyanine dyads, S^* has been assigned in the target analysis as an independent intermediate electronic excited state between S_2 and S_1 [11]. However, coupling between the chromophores in the carotenoid zinc phthalocyanine dyads is apparent, since in the dyad, the carotenoid S_1 lifetime is reduced from that of the free carotenoid [11]. We do not observe such an effect in the caroteno-purpurin dyad and the carotenoid S_1 lifetime is more or less unaffected by the linking to the purpurin. Hence, deviations in the deactivation pathways between these two related dyad systems might have their origin in the different couplings between their constituents. Although, we find no motive to exclude the $HotS_1$ state of the carotenoid from the target analysis [24] as was done by Berera et al. [11].

(c) *Hot ground state model.* In accordance with our previous work on carotenoids [3,16] and the artificial light-harvesting complex [24], we now assume that the so-called S^* signal belongs to a hot ground state that is populated by impulsive Raman scattering. In the proposed hot ground state model, the additional contributions are assigned to a vibrationally hot ground state ($HotS_0$, Fig. 6c) rather than to the suggested additional excited electronic states or photoisomerization products.

The spectro-temporal signal on the red side of the ground state absorption band depicts several characteristics that are in line with the hot ground state hypothesis. First, the maximum of this signal is red shifted with respect to the $S_0 \rightarrow S_2$ absorption, as expected for a vibrationally hot ground state. Second, studies varying the length of the carotenoid [5,21,16] show that its relaxation time differs from that of the S_1 state, and does not follow the energy gap rule [34], which illustrates the characteristics of a vibrationally hot state rather than an electronic excited state. Furthermore, the signal is located exactly where the fluorescence (or stimulated emission) signal from S_2 appears [24] indicating a favourable transition, which makes this transition a very likely candidate for the extra excitation channel found in the dyad molecule. In a previous study, we showed how, by tuning the excitation wavelength, the ISRS process to the Hot S_0 could be enhanced by some 28% in a β-carotenoid derivative with 15 conjugated double bonds [16]. This finding is in line with the observations in all-*trans*-neurosporene [35], where it was shown that the stimulated emission was strongly affected when the pump excitation was moved from vibrational sub-band 0–0 to 0–1 in the $S_0 \rightarrow S_2$ transition. The emission 1–1 could be enhanced and 1–2 decreased when S_2 was pumped at $v = 1$, which is actually just a result of a better Franck–Condon factor, mirroring the displacement of S_0 and S_2 potential surfaces. The importance of the electronic resonance for ISRS in β-carotene has also been demonstrated in a coherent control experiment [36]. Also, similar enhancement of the S^* signal has been observed by Billsten et al. [20]. In this study also excitation in the UV was tested, thus addressing a higher density of states by the pump pulse. Presumably, this leads to a better starting condition for the second (dumping) step in the suggested two-photon process.

A puzzle remains regarding the non-quadratic behaviour of the population of the $HotS_0$ as a function of the input pulse energy. To address this point, we performed an analysis using the density-matrix formalism. This analysis is based on the Liouville formulation of quantum mechanics, which considers the density-matrix (as opposed to wavefunction) as the unknown function, and does not make approximations based on perturbation theory. Details of the technique and its application to quantum control spectroscopy can be found in an earlier publication [37]. Briefly, the diagonal elements of the density-matrix determine populations of the different levels, while the off-diagonal elements represent electronic and vibrational coherences. The excitation of a low-lying state (such as a hot ground state) requires the interaction of two-photons with the system. We therefore considered here a 3 + 1 level system consisting of three levels in a Λ-configuration (levels S_0, S_2 and Hot S_0), together with a fourth level (S_1), which is coupled through incoherent processes, as shown in Fig. 7a. The system results in a set of 10 real nonlinear first-order coupled differential equations. Our approach considers the rotating-wave approximation [38] with the envelope of the laser electric field being a direct input to the system. We note that the aim of the following study is to understand the intensity dependence of the reported data in the context of the hot ground state model, and not a comprehensive description of complex molecular systems like the artificial light-harvesting dyad.

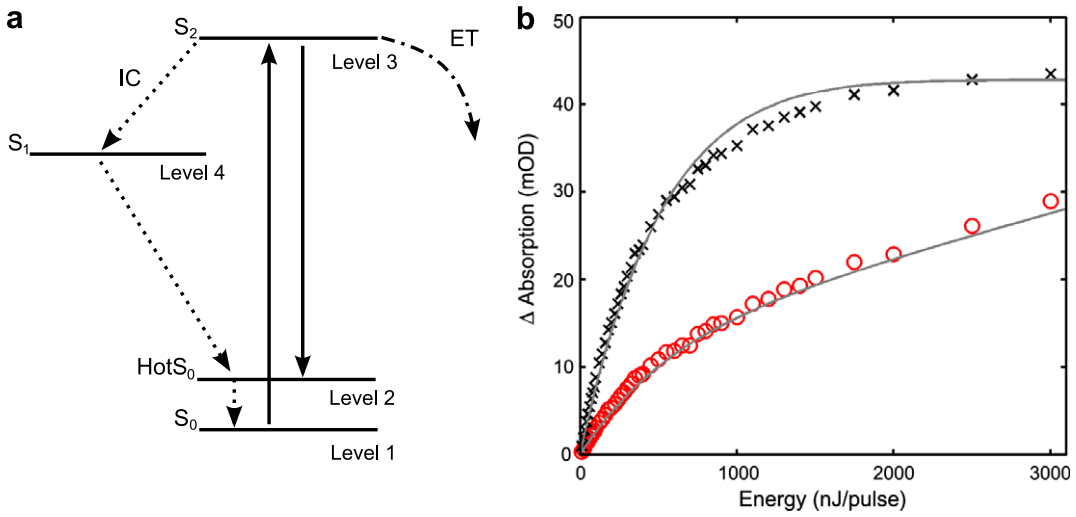

Fig. 7. Density-matrix model and results. (a) The energy-level diagram used in the simulations. (b) The amplitude factors from the SAS-fit of the experimental results: $HotS_0$ (red circles) and S_1 (black crosses), and corresponding simulations using the density-matrix analysis (grey lines).

Simulation parameters were set as follows (see the energy-level diagram in Fig. 7a). The energy spacing between S_0 and $HotS_0$ was chosen as 1090 cm^{-1} corresponding to the energy difference between the absorption maxima of the $HotS_0$ and the lowest energy maximum of the linear absorption spectrum. The separation between S_0 and S_2 was chosen as 19,608 cm^{-1} (the centre of the used pump pulse spectrum, 510 nm). Population relaxation times (T_1's) associated with S_2 were set at 50 fs and 110 fs for the ET and IC channels, respectively [24]. Population relaxation times associated with S_1 and $HotS_0$ were both set at 7.0 ps [24]. Further, an electronic dephasing time (T_2) of 2 fs, a vibrational dephasing time of 1 ps, and a relative dipole value of $\mu_{23}/\mu_{13} = 0.19$ were used. Note that a relatively fast electronic dephasing needs to be considered in order to avoid coherent Rabi oscillations and to obtain the observed saturation. It is also worth noting that an asymmetric Λ-transition is considered in the model, with different strengths for the coupling between the two dipole-allowed transitions. In particular, the simulations predict different strengths of the coupling between the two dipole-allowed transitions; the coupling between S_0 and S_2 is roughly five times that of the coupling between S_2 and $HotS_0$.

Fig. 7b shows the simulated and measured populations of the $HotS_0$ and S_1 levels for different input pulse energies. Simulations are in good agreement with the experimental results, both in the low-energy and high-energy regimes. Contrary to what one would expect for a two-photon transition, the pulse energy dependence of the $HotS_0$ signal, shown in Fig. 7b, is not quadratic. Indeed, the energy dependence originates from the initial two-photon resonance $S_0 \rightarrow S_2 \rightarrow HotS_0$. In this case, however, ISRS is not the only process populating level $HotS_0$, since the decay from S_1 also contributes and therefore influences the observed two-photon energy dependence. Finally, we note that the simulations here were used to investigate whether the missing two-photon dependence of the $HotS_0$ could be qualitatively modelled using the density-matrix approach. Considering the scope of this contribution we leave out results from more extensive simulations as well as more extensive discussion, which will be presented in a future study.

5. Conclusions

We used an artificial light-harvesting dyad in order to study the carotenoid excited state dynamics by varying the pump pulse energy in a transient absorption experiment. Different features of the transient absorption data show varying responses to the pump energy-level. These results are analysed by fitting previously resolved SAS as well as using a density-matrix formalism. The behaviour of transient signals, as well as previously resolved SAS, are best explained with a kinetic model including a hot ground state that is populated within the excitation pulse by ISRS. Even at relatively moderate intensities and partly saturated signals, a good analysis of the data requires neither additional dark states nor pathways involving multi-photon transfer to higher states in the artificial light-harvesting complex. We conclude that the only necessary addition to the classical three-level energy-flow diagram is the hot ground state. This is strongly supported by analysis of experimental data. The dyad confirms its value as a good model system for such fundamental studies, as it endures higher pulse energies than natural light-harvesting complexes. Furthermore, this study shows that the interpretation of transient absorption results can greatly benefit from thorough energy dependence measurements and analysis.

Acknowledgements

We are grateful to P. Liddell, D. Gust, T.A. Moore, and A. Moore for providing the caroteno-purpurin dyad. This work is part of the research program of the "Stichting voor Fundamenteel Onderzoek der Materie (FOM)", which is financially supported by the "Nederlandse organisatie voor Wetenschappelijk Onderzoek (NWO)". CS acknowledges support from the Spanish Ministry of Education and Science through Project FIS2008-06368-C02-02.

References

[1] T. Polivka, V. Sundström, Chem. Rev. 104 (2004) 2021.
[2] E. Papagiannakis, J.T.M. Kennis, I.H.M. van Stokkum, R.J. Cogdell, R. van Grondelle, Proc. Natl. Acad. Sci. USA 99 (2002) 6017.
[3] W. Wohlleben, T. Buckup, H. Hashimoto, R. Cogdell, J. Herek, M. Motzkus, J. Phys. Chem. B 108 (2004) 3320.
[4] E. Papagiannakis, I.H.M. van Stokkum, M. Vengris, R.J. Cogdell, R. van Grondelle, D.S. Larsen, J. Phys. Chem. B 110 (2006) 5727.
[5] D.M. Niedzwiedzki, J.O. Sullivan, T. Polivka, R.R. Birge, H.A. Frank, J. Phys. Chem. B 110 (45) (2006) 22872.
[6] P. Tavan, K. Schulten, J. Chem. Phys. 85 (11) (1986) 6602.
[7] P. Tavan, K. Schulten, Phys. Rev. B: Condens. Matter Mater. Phys. 36 (8) (1987) 4337.
[8] R. Fujii, T. Inaba, Y. Watanabe, Y. Koyama, J.P. Zhang, Chem. Phys. Lett. 369 (2003) 165.
[9] G. Cerullo, D. Polli, G. Lanzani, S. De Silvestri, H. Hashimoto, R.J. Cogdell, Science 298 (2002) 2395.
[10] M. Ikuta, A. Yabushita, F.S. Rondonuwu, J. Akahane, Y. Koyama, T. Kobayashi, Chem. Phys. Lett. 422 (2006) 95.
[11] R. Berera, I.H.M. van Stokkum, G. Kodis, A.E. Keirstead, S. Pillai, C. Herrero, R.E. Palacios, M. Vengris, R. van Grondelle, D. Gust, T.A. Moore, A.L. Moore, J.T.M. Kennis, J. Phys. Chem. B 111 (24) (2007) 6868.
[12] C.C. Gradinaru, J.T.M. Kennis, E. Papagiannakis, I.H.M. van Stokkum, R.J. Cogdell, G.R. Fleming, R.A. Niederman, R. van Grondelle, Proc. Natl. Acad. Sci. USA 98 (2001) 2364.
[13] W. Wohlleben, T. Buckup, J.L. Herek, R.J. Cogdell, M. Motzkus, Biophys. J. 85 (2003) 442.
[14] J. Hauer, T. Buckup, M. Motzkus, J. Phys. Chem. A 111 (2007) 10517.
[15] Y. Koyama, F.S. Rondonuwu, R. Fujii, Y. Watanabe, Biopolymers 74 (2004) 2.
[16] T. Buckup, J. Savolainen, W. Wohlleben, J.L. Herek, H. Hashimoto, R.R.B. Correia, M. Motzkus, J. Chem. Phys. 125 (2006) 194505.
[17] D. Kosumi, M. Komukai, H. Hashimoto, M. Yoshizawa, Ultrafast dynamics of all-trans-β-carotene explored by resonant and nonresonant photoexcitations, Phys. Rev. Lett., p. 95.
[18] J.L.P. Lustres, D. Alexander, L. Dobryakov, A. Holzwarth, M. Veiga, Angew. Chem. Ed. 46 (2007) 3758.
[19] P. Kukura, D.W. McCamant, R.A. Mathies, J. Phys. Chem. A 108 (28) (2004) 5921.
[20] H.H. Billsten, J. Pan, S. Sinha, T. Pascher, V. Sundström, T. Polívka, J. Phys. Chem. A 109 (31) (2005) 6852.
[21] D. Niedzwiedzki, J.F. Koscielecki, H. Cong, J.O. Sullivan, G.N. Gibson, R.R. Birge, H.A. Frank, J. Phys. Chem. B 111 (21) (2007) 5984.
[22] H. Cong, D.M. Niedzwiedzki, G.N. Gibson, H.A. Frank, J. Phys. Chem. B 112 (11) (2008) 3558.
[23] P.O. Andersson, T. Gillbro, J. Chem. Phys. 103 (1995) 2509.
[24] J. Savolainen, N. Dijkhuizen, R. Fanciulli, P.A. Liddell, D. Gust, T.A. Moore, A.L. Moore, J. Hauer, T. Buckup, M. Motzkus, J.L. Herek, J. Phys. Chem. B 112 (2008) 2678.
[25] D. Gust, T.A. Moore, A.L. Moore, Acc. Chem. Res. 34 (2001) 40.
[26] D. Gust, T.A. Moore, A.L. Moore, Acc. Chem. Res. 26 (1993) 198.
[27] D. Gust, T.A. Moore, A.L. Moore, C. Devadoss, P.A. Liddell, R. Hermant, R.A. Nieman, L.J. Demanche, J.M. DeGraziano, I. Gouni, J. Am. Chem. Soc. 114 (1992) 3590.
[28] R. Berera, C. Herrero, L.H.M. van Stokkum, M. Vengris, G. Kodis, R.E. Palacios, H. van Amerongen, R. van Grondelle, D. Gust, T.A. Moore, A.L. Moore, J.T.M. Kennis, Proc. Natl. Acad. Sci. USA 103 (2006) 5343.
[29] J. Savolainen, R. Fanciulli, N. Dijkhuizen, A.L. Moore, J. Hauer, T. Buckup, M. Motzkus, J.L. Herek, Proc. Natl. Acad. Sci. USA 105 (22) (2008) 7641.
[30] A. Macpherson, P. Liddell, D. Kuciauskas, D. Tatman, T. Gillbro, D. Gust, T. Moore, A. Moore, J. Phys. Chem. B 106 (2002) 9424.
[31] T. Ye, N. Friedman, Y. Gat, G. Atkinson, M. Sheves, M. Ottolenghi, S. Ruhman, J. Phys. Chem. B 103 (24) (1999) 5122.
[32] B. Hou, N. Friedman, S. Ruhman, M. Sheves, M. Ottolenghi, J. Phys. Chem. B 105 (29) (2001) 7042. doi:10.1021/jp0034980.
[33] D. Polli, G. Cerullo, G. Lanzani, S. De Silvestri, K. Yanagi, H. Hashimoto, R.J. Cogdell, Phys. Rev. Lett. 93 (2004) 163002.
[34] R. Englman, J. Jortner, Mol. Phys. 18 (2) (1970) 145.
[35] J.P. Zhang, T. Inaba, Y. Watanabe, Y. Koyama, Chem. Phys. Lett. 331 (2000) 154.
[36] J. Hauer, H. Skenderovic, K.L. Kompa, M. Motzkus, Chem. Phys. Lett. 421 (2006) 523.
[37] T. Buckup, J. Hauer, C. Serrat, M. Motzkus, J. Phys. B: At., Mol. Opt. Phys. 41 (2008) 074012.
[38] E.T. Jaynes, F.W. Cummings, Proc. IEEE 51 (1) (1963) 89.